

LETTER • OPEN ACCESS

A miniaturized 4 K platform for superconducting infrared photon counting detectors

To cite this article: Nathan R Gemmell *et al* 2017 *Supercond. Sci. Technol.* **30** 11LT01

View the [article online](#) for updates and enhancements.

Related content

- [Superconducting nanowire single-photon detectors: physics and applications](#)
Chandra M Natarajan, Michael G Tanner and Robert H Hadfield
- [Performance of Superconducting Nanowire Single-Photon Detection System](#)
Shen Xiao-Fang, Yang Xiao-Yan and You Li-Xing
- [Traceable calibration of a fibre-coupled superconducting nano-wire single photon detector using characterized synchrotron radiation](#)
Ingmar Müller, Roman M Klein and Lutz Werner



 **can
superconductors**

www.can-superconductors.com

HTS PARTS AND MATERIALS

Single and Multi-domain YBCO Bulk
REBCO Sputtering Targets
REBCO Powders and Granulates
BSCCO Current Leads, Magnetic Shields
Superconductivity Demonstration Kits

Letter

A miniaturized 4 K platform for superconducting infrared photon counting detectors

Nathan R Gemmell¹, Matthew Hills², Tom Bradshaw², Tom Rawlings², Ben Green², Robert M Heath¹, Konstantinos Tsimvraakis¹, Sergiy Dobrovolskiy³, Val Zwiller^{3,4}, Sander N Dorenbos³, Martin Crook² and Robert H Hadfield¹

¹School of Engineering, University of Glasgow, Glasgow, G12 8QQ, United Kingdom

²STFC Rutherford Appleton Laboratory, Harwell Campus, Didcot, OX11 0QX, United Kingdom

³Single Quantum B.V., 2628 CH Delft, The Netherlands

⁴Department of Applied Physics, Royal Institute of Technology (KTH), SE-106 91 Stockholm, Sweden

E-mail: Robert.Hadfield@glasgow.ac.uk

Received 19 July 2017, revised 26 August 2017

Accepted for publication 6 September 2017

Published 29 September 2017



CrossMark

Abstract

We report on a miniaturized platform for superconducting infrared photon counting detectors. We have implemented a fibre-coupled superconducting nanowire single photon detector in a Stirling/Joule–Thomson platform with a base temperature of 4.2 K. We have verified a cooling power of 4 mW at 4.7 K. We report 20% system detection efficiency at 1310 nm wavelength at a dark count rate of 1 kHz. We have carried out compelling application demonstrations in single photon depth metrology and singlet oxygen luminescence detection.

Keywords: cooling, superconducting nanowire single photon detectors, superconducting devices, SOLD, LiDAR, single photon detectors

(Some figures may appear in colour only in the online journal)

1. Introduction

Superconducting nanowire single photon detectors (SNSPDs) [1] have rapidly advanced to the forefront of infrared photon counting technology. Optical fibre-coupled single pixel SNSPD devices [2] have been demonstrated to offer near unity 1550 nm wavelength single photon detection efficiency [3, 4], low timing jitter [5] (<18 ps FWHM), low intrinsic dark count rate [6] (mHz), and high count rates [7] far outperforming alternative technologies such as semiconductor (InGaAs/InP) based single photon avalanche diodes and photomultipliers [8].

Furthermore, SNSPDs have been shown to be capable of single photon detection at wavelengths up to 5 μm [9], well beyond the InGaAs cut-off at 1.7 μm . These properties make them the ideal detectors for the continued development of a wide range of emerging applications, including fundamental tests of quantum mechanics [10], space to ground communications [11], long range 3D infrared depth imaging [12], integrated circuit testing [13], quantum key distribution [14], fibre optic temperature sensing [15], and singlet oxygen luminescence detection [16]. However, their deployment outside of the laboratory has remained hindered by the cooling requirements. Although the need for liquid cryogenics has been eliminated by the use of practical closed-cycle cryocoolers [17–20], such bulky, power hungry systems are not truly capable of mobile operation. Interest is increasing in engineering new solutions for compact closed-cycle cooling for 4 K [21, 22] and below.

 Original content from this work may be used under the terms of the [Creative Commons Attribution 3.0 licence](https://creativecommons.org/licenses/by/3.0/). Any further distribution of this work must maintain attribution to the author(s) and the title of the work, journal citation and DOI.

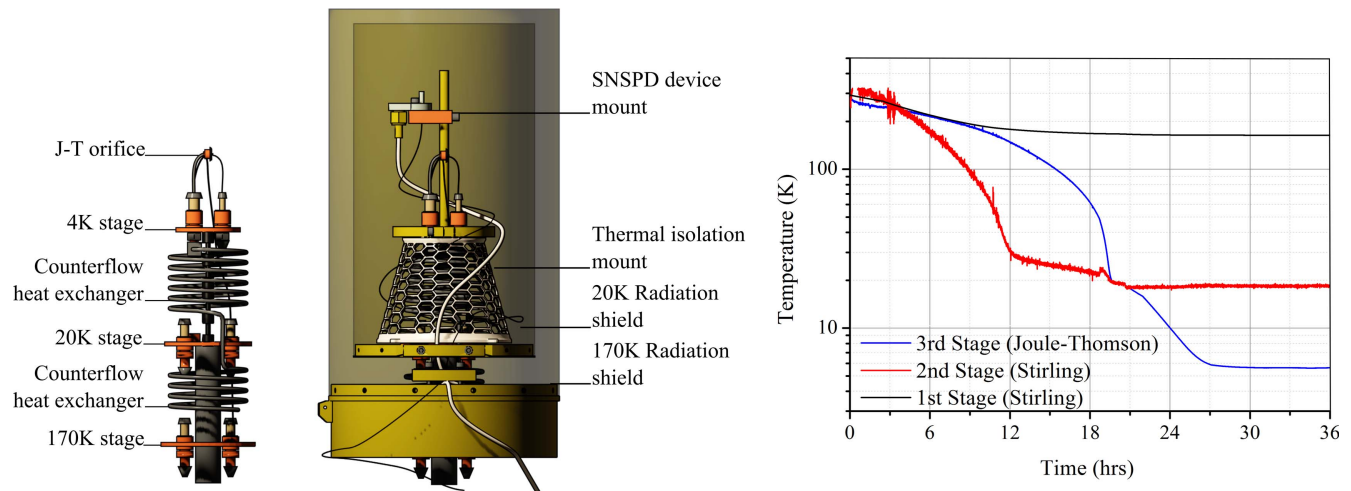


Figure 1. Left: schematic of cold finger mechanism alongside the cryostat design with new parts for SNSPD mounting added. Right: typical cool-down plot for the three cold finger stages: 1st Stage (Stirling), 2nd Stage (Stirling) and 3rd Stage (Joule–Thomson).

Here we present a fully closed-cycle miniaturised cooling platform based on Stirling and Joule–Thomson (J–T) cycles (with ^4He gas) to reach a base temperature of 4.2 K. The system was originally designed as a demonstrator for the Planck space mission [23, 24]. A functionally equivalent version of the J–T cooler used in this system went on to be launched aboard an Ariane 5 rocket in 2009 as part of the Planck spacecraft [25], and operated flawlessly for the entire mission duration of nearly 4.5 years (>39 k h). Our platform has been refitted specifically to house SNSPDs, and here we demonstrate the operation of a fibre-coupled single pixel detector with 20% system detection efficiency at 1310 nm wavelength.

2. Experimental

2.1. J–T Stirling cooler design

Figure 1 shows the configuration of the cold stages. The first two stages on the Stirling cooler reach 170 and 20 K while the third J–T stage allows the base temperature of 4.2 K to be achieved. Provision is made on the Stirling cooler stages for heat sinking the detector’s coax cable by clamping the outer shield to the copper stage. This reduces the heat load on the J–T stage to a level where it has minimal effect of the cooling available at 4.2 K. The third stage is attached to the others via a 3D printed mount (constructed from VeroGrey), giving structural stability with a low thermal conductance. A J–T by-pass system diverts gas flow past the third (J–T) heat exchanger and the orifice. This acts as a thermal switch, thermally connecting the final stage to the coldest stage of the Stirling pre-cooler. When the temperature of the final stage is close to that of the pre-cooler the by-pass system is deactivated; ^4He gas flow is then directed through the orifice and J–T cooling starts.

The cold stages are contained within a small cryostat that was specifically configured for use with SNSPDs. The base of the vacuum vessel consists of a manifold flange which

provides feedthroughs for temperature sensors, detector coax cables, optical fibres and a vacuum port. The upper part of the vessel seals to the manifold flange using an o-ring and quick release clamp band to allow rapid access for detector changes. The cryostat is continually pumped using a Leybold Turbovac80. Radiation shields attached to the two stages of the Stirling cooler reduce the heat load to the final stage, which is minimised further by the addition of Multi-Layer Insulation to these shields.

Both the Stirling and J–T coolers employ long-life, linear compressors developed for space applications. The long life of these devices comes from the use of flexure bearings which are operated well within the fatigue failure limit of the material. The compressors are reciprocating and the flexure bearings are used to support the pistons. The pistons are non-contacting and non-lubricated and are operated at 30–50 Hz which limits the ‘DC’ gas leakage. The gas in the J–T system is circulated through a gas panel which contains pressure transducers, a mass flow meter and a getter. The getter removes contaminants from the ^4He gas which might block the orifice on the J–T stage. Additional filters on each of the cold stages also help to clean the gas prior to expansion. These measures are necessary as the orifice size is only approximately $12\ \mu\text{m}$. The mechanisms have undergone mechanical tests appropriate for an Ariane 5 launch.

The cooler provides around 6 mW of cooling power at 4.2 K which is appropriate for the type of work on SNSPDs. The total input power to the cooler mechanisms is around 130 W. The weight of the compressors is approximately 14 kg, while the displacer and momentum compensator are 6 kg, and the plumbing adds a further 2 kg. This is currently housed in a 34 kg frame designed for vibration testing (the size and weight of the frame could be significantly reduced). Further designs could easily see such a cooler fit into a standard 19" rack.

The detector cryostat was designed to operate as a complete standalone demonstrator (unveiled at the UK Quantum Technology Showcase in Westminster, London UK on 3rd November 2016 [26]). The cryostat/cold-head/compressor (approximate base dimension 55 cm by 55 cm, height 63 cm) is

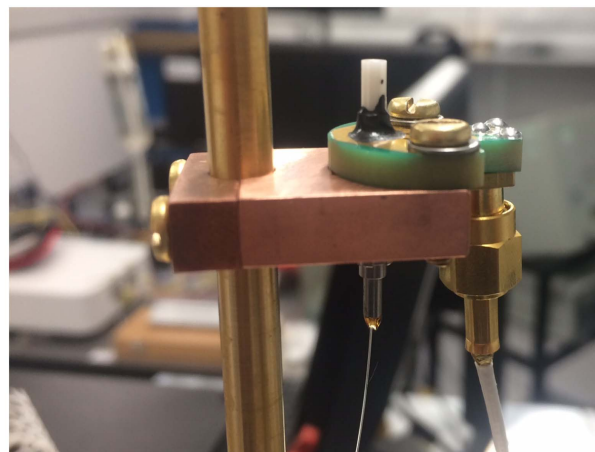
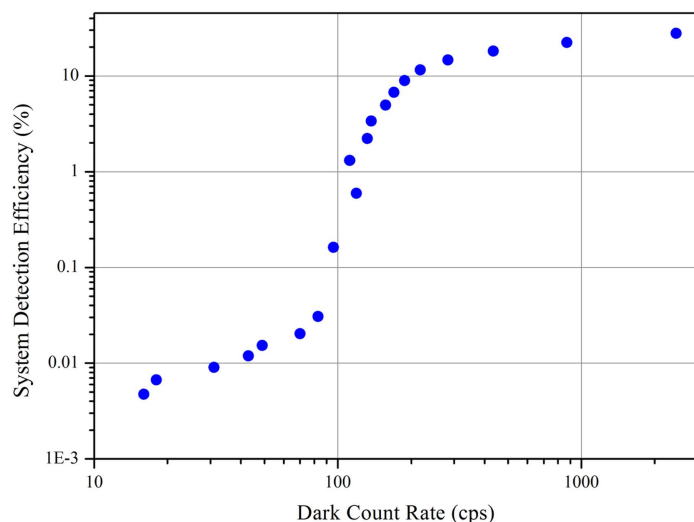


Figure 2. Left: single photon detection efficiency measured from the fibre optic input of our system, as a function of dark count rate, showing a peak efficiency of $>20\%$ at 1310 nm wavelength. Right: photograph of fibre-coupled SNSPD device mounted at the 4 K stage in the miniature cooler.

integrated into a moveable base platform incorporating turbo pump, water chiller, system electronics and control PC) (footprint 102×122 cm) operating from standard 13 A 230 V mains power.

2.2. SNSPD

A NbTiN single meander SNSPD in an optical cavity (optimized for 1310 nm wavelength) was housed in the cryostat and attached via self-alignment to $9 \mu\text{m}$ core single mode optical fibre (entering the cooler through an epoxied feed-through). The SNSPD is biased via a Stanford Research Systems SIM900 rack (SIM928 battery powered voltage source and $100 \text{ k}\Omega$ load resistor) through a bias tee and operated with a 50Ω shunt resistor (to avoid latching at higher bias). Two room-temperature RF-Bay LNA-1000 amplifiers (each 33 dB gain, 10–1000 MHz range, 2 dB noise figure) amplify the signal peaks ready for counting equipment. The critical current of the device was measured to be $8.5 \mu\text{A}$ at 3 K, and $6 \mu\text{A}$ at 4.2 K.

3. Results and discussion

3.1. Performance test of cooler

The cooler temperatures during a typical cool-down are plotted in figure 1 (right), showing the total time from room to base temperature is <30 h. Temperature fluctuations of the order 10 mK are observed over a time frame of several hours, and are linked to temperature variations within the ambient laboratory space. Preliminary tests to baseline the cooler performance were made before the adaptations for the SNSPDs were implemented. In these tests, the 4 K stage reached a stable base temperature of 4.8 K. The available cooling power is measured by applying a large heat load to the 4 K stage for sufficient time to boil off any ^4He liquid that

has formed in the reservoir downstream of the J–T orifice. Once the liquid has evaporated, the temperature of the stage starts to rise and the applied heat load is reduced. If the stage then returns to a stable base temperature, the available cooling power is in excess of the applied load at this temperature. Finding the maximum available cooling power is therefore an iterative process with the aim being to reduce the heat load to a value that is just below the maximum heat that the cooler can remove. Using this method, the available cooling power in this configuration was found to be approximately 3 mW at 4.8 K.

Further performance tests were conducted once the modifications required to accommodate the SNSPDs had been made to the cryostat. With these changes implemented and with a detector coax cable running to the 4 K stage—but without a detector fitted—a cooling power of 4 mW at approximately 4.7 K was achieved. The slightly improved performance in this configuration is attributed to a modification to the cooler drive electronics that allowed the J–T compressors to be driven closer to their maximum strokes. Further stroke margin was still available, so it is anticipated that higher cooling powers are possible, offering the potential to run the system with multiple SNSPDs.

3.2. Detector characterization

Single photon efficiency tests were performed at 1310 nm (the peak design wavelength of the SNSPD optical cavity), with the cooler operating at 4.3 K, with system detection efficiency at the input of the cooler shown in figure 2. An efficiency of $>20\%$ at kHz dark count rate is demonstrated, with polarization controlled to achieve maximum efficiency. This corresponds with initial tests performed using conventional cooling methods, which gave detection efficiencies of 21% at 4.2 K (liquid ^4He) and 30% at 3 K (closed cycle). Timing jitter was measured using a 50 MHz repetition frequency, ps pulse width 1560 nm fibre laser. Detector response was

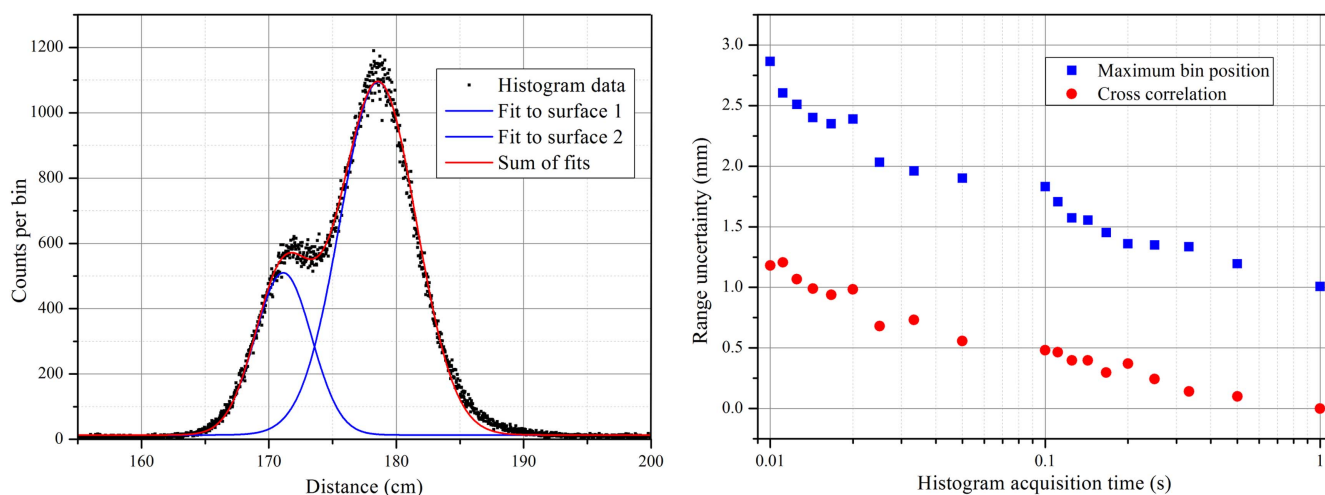


Figure 3. Left: histogram of photon returns from a test target consisting of a clear plastic plane in front of a black plastic plane. Right: range uncertainty (calculated as the standard deviation of peak position for 100 histograms) as a function of acquisition time, using both unprocessed histograms and the same histograms processed with a cross-correlation function.

recorded on a time correlated single photon counting (TCSPC) module (PicoQuant HydraHarp). A measured FWHM timing jitter of ~ 200 ps suggests that electrical noise within the system could be mitigated with improved system design and device isolation.

3.3. NaN Single photon Light Detection and Ranging (LIDAR) at 1560 nm

Infrared single photon measurements allow long range eye-safe range-finding and imaging, and are an enabling technology for future transformative applications such as driverless cars [27]. In 2013 a kilometre range depth imaging system using SNSPDs was demonstrated [8], producing fast target profiles in broad daylight conditions with eye-safe laser levels. Such a system combined with this miniaturized cooling platform would be capable of mobile deployment on ground based vehicles or even in aircraft for high speed target identification or terrain mapping.

Here we demonstrate a simple LIDAR experiment using a coaxial transmit and return beam path split by a mirror with a hole. A 1.5 mW average power, 50 MHz repetition rate, 1560 nm wavelength fibre laser is used as the illumination source. Laser sync and SNSPD outputs are sent to the same TCSPC module as in the jitter measurements to time-stamp photon arrival times, relative to the laser repetition rate. The left side of figure 3 shows an example of overlapping peaks from a beam path obstructed by two uncooperative plastic targets, the first clear plastic and the second black plastic at 1.5 m distance. Range uncertainty as a function of histogram acquisition time is also shown for a single peak taken from the black plastic target. The uncertainty (right of figure 3) is calculated from the standard deviation of peak position from 100 histograms at each acquisition time. Uncertainty data is shown for both unprocessed histograms, as well as for histograms processed through a simple cross correlation with an instrumental response as described in [8].

3.4. NaN.1 Singlet oxygen luminescence detection

The detection of an infrared photon at a wavelength of 1270 nm is the signature of singlet oxygen. This excited oxygen state plays a key role in many biological and physiological processes. SNSPDs have previously been shown to be capable of detecting this very weak transition [10], which is crucial in direct dose monitoring for photodynamic therapy (PDT) in the treatment of cancer. In PDT the photosensitiser treatment drug (typically a dye molecule) exchanges energy with surrounding oxygen molecules on optical excitation, creating singlet oxygen radicals which kill tumour cells. A miniaturised cooling platform such as that presented here would make SNSPD use in Singlet Oxygen Luminescence Dosimetry in clinical PDT significantly more practical.

The histograms shown in figure 4 demonstrate the ability of this system to detect the weak 1270 nm signal (a 1300 nm is shown for comparison). This data was taken from a standard photosensitiser dye (Rose Bengal, $250 \mu\text{g ml}^{-1}$), illuminated by a 0.4 mW, 24 kHz laser at 540 nm wavelength with 100 nm spectral bandwidth (this marks the maximum absorption peak of this photosensitiser sample).

4. Conclusions

We have successfully demonstrated a SNSPD integrated into a next generation miniaturized closed-cycle cooling platform. The cryostat combines a two-stage Stirling cooler with a J-T stage, allowing a base temperature of 4.2 K to be reached for continuous operation. Heat load measurements verify a maximum cooling power of >4 mW. We have mounted an optical fibre-coupled SNSPD in the system, achieving 20% system detection efficiency at 1310 nm wavelength and 200 ps FWHM timing jitter. This performance has enabled us to execute demonstration experiments in advanced infrared photon counting applications, namely infrared single photon LIDAR and singlet oxygen luminescence detection.

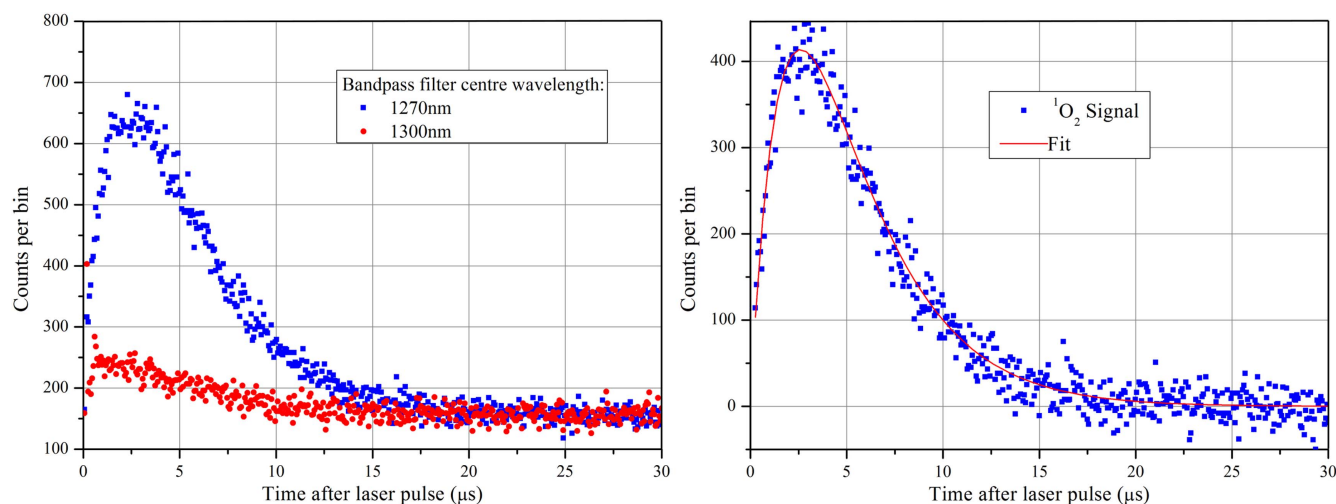


Figure 4. Left: histograms taken from the singlet oxygen luminescence set up, using both a 1270 and 1300 nm band pass filters. Right: fitting of a double exponential (as described in [16]) gives lifetimes of the triplet state of the Rose Bengal ($2.0 \pm 0.1 \mu\text{s}$) and of the singlet oxygen ($3.4 \pm 0.2 \mu\text{s}$).

We anticipate future systems based on this demonstrator could accommodate larger numbers of SNSPD detectors and SNSPD arrays and could be deployed in a wide range of real world scenarios. Moreover, this robust flexible miniature 4 K cooler could offer a mobile platform for superconducting electronics and a wide range of other low temperature quantum technologies [19].

Acknowledgments

The authors acknowledge support through QuantIC, the UK Quantum Technology Hub in Quantum Enhanced Imaging (Engineering and Physical Sciences Research Council grant EP/M01326X/1). We thank Single Quantum for supplying a sample SNSPD device. RHH acknowledges a European Research Council Consolidator Grant (IRIS 648604). MH, TB, TR and MC acknowledge previous and ongoing support from the European Space Agency (ESA) and the UK Science and Technology Facilities Council (STFC).

References

- [1] Gol'tsman G N, Okunev O, Chulkova G, Lipatov A, Semenov A, Smirnov K, Voronov B, Dzardanov A, Williams C and Sobolewski R 2001 Picosecond superconducting single-photon optical detector *Appl. Phys. Lett.* **79** 705–7
- [2] Dauler E A, Grein M E, Kerman A J, Marsili F, Miki S, Nam S W, Shaw M D, Terai H, Verma V B and Yamashita T 2014 Review of superconducting nanowire single-photon detector system design options and demonstrated performance *Opt. Eng.* **53** 081907
- [3] Marsili F *et al* 2013 Detecting single infrared photons with 93% system efficiency *Nat. Photon.* **7** 210–4
- [4] Zwiller V, Esmail Zadeh I, Los J, Gourgues R, Steinmetz V, Dobrovolskiy S, Dorenbos S N and Dorenbos S N 2017 Single-photon detection with near unity efficiency, ultra-high detection-rates, and ultra-high time resolution *Conf. on Lasers and Electro-Optics* p FF1E.1
- [5] Shcheslavskiy V, Morozov P, Divochiy A, Vakhtomin Y, Smirnov K and Becker W 2016 Ultrafast time measurements by time-correlated single photon counting coupled with superconducting single photon detector *Rev. Sci. Instrum.* **87** 053117
- [6] Schuck C, Pernice W H P and Tang H X 2013 Waveguide integrated low noise NbTiN nanowire single-photon detectors with milli-Hz dark count rate *Sci. Rep.* **3** 1893
- [7] Zadeh I E, Los J W N, Gourgues R B M, Steinmetz V, Bulgarini G, Dobrovolskiy S M, Zwiller V and Dorenbos S N 2016 Single-photon detectors combining ultra-high efficiency, detection-rates, and timing resolution arXiv:1611.02726
- [8] Hadfield R H 2009 Single-photon detectors for optical quantum information applications *Nat. Photon.* **3** 696–705
- [9] Marsili F, Bellei F, Najafi F, Dane A E, Dauler E A, Molnar R J and Berggren K K 2012 Efficient single photon detection from 500 nm to $5 \mu\text{m}$ wavelength *Nano Lett.* **12** 4799–804
- [10] Shalm L K *et al* 2015 Strong loophole-free test of local realism *Phys. Rev. Lett.* **115** 250402
- [11] Grein M E, Kerman A J, Dauler E A, Willis M M, Romkey B, Molnar R J, Robinson B S, Murphy D V and Boroson D M 2015 An optical receiver for the lunar laser communication demonstration based on photon-counting superconducting nanowires *Proc. SPIE* **9492** 949208
- [12] McCarthy A, Krichel N J, Gemmell N R, Ren X, Tanner M G, Dorenbos S N, Zwiller V, Hadfield R H and Buller G S 2013 Kilometer-range, high resolution depth imaging via 1560 nm wavelength single-photon detection *Opt. Express* **21** 8904
- [13] Zhang J *et al* 2003 Noninvasive CMOS circuit testing with NbN superconducting single-photon detectors *Electron. Lett.* **39** 1086
- [14] Takesue H, Nam S W, Zhang Q, Hadfield R H, Honjo T, Tamaki K and Yamamoto Y 2007 Quantum key distribution over a 40 dB channel loss using superconducting single-photon detectors *Nat. Photon.* **1** 343–8

- [15] Tanner M G, Dyer S D, Baek B, Hadfield R H and Nam S W 2011 High-resolution single-mode fiber-optic distributed Raman sensor for absolute temperature measurement using superconducting nanowire single-photon detectors *Appl. Phys. Lett.* **99** 201110
- [16] Gemmell N R, McCarthy A, Liu B, Tanner M G, Dorenbos S D, Zwiller V, Patterson M S, Buller G S, Wilson B C and Hadfield R H 2013 Singlet oxygen luminescence detection with a fiber-coupled superconducting nanowire single-photon detector *Opt. Express* **21** 5005–13
- [17] Natarajan C M, Tanner M G and Hadfield R H 2012 Superconducting nanowire single-photon detectors: physics and applications *Supercond. Sci. Technol.* **25** 63001
- [18] Radenbaugh R 2004 Refrigeration for superconductors *Proc. IEEE* **92** 1719–34
- [19] Seidel P 2015 *Applied Superconductivity: Handbook on Devices and Applications* (New York: Wiley)
- [20] Hadfield R H, Habif J L, Schlafer J, Schwall R E and Nam S W 2006 Quantum key distribution at 1550 nm with twin superconducting single-photon detectors *Appl. Phys. Lett.* **89** 241129
- [21] Kotsubo V, Radebaugh R, Hendershott P, Bonczyski M, Wilson B, Nam S W and Ullom J N 2017 Compact 2.2 K cooling system for superconducting nanowire single photon detectors *IEEE Trans. Appl. Supercond.* **27** 1–5
- [22] This preliminary report is of a pulse tube/JT design reaching a base temperature of 2.2 K without a detector mounted.
- [23] Planck. http://esa.int/Our_Activities/Space_Science/Planck (accessed: 29 Jan 2016)
- [24] <http://sci.esa.int/planck/45498-cooling-system/?fbodylongid=2124>
- [25] Perez E 2004 Ariane 5 Users Manual, no. 4
- [26] EPSRC, Quantum Technologies Showcase. <https://epsrc.ac.uk/newsevents/news/quantumtechshowcase2016launch/>
- [27] Waldrop M M 2015 Autonomous vehicles: no drivers required *Nature* **518** 20–3